

# The Critical Accommodation Coefficient for Velocity Inversion in Rarefied Cylindrical Couette Flow in the Slip and Near Free-Molecular Regimes

S. K. Stefanov<sup>1</sup>, R. W. Barber<sup>2</sup>, D. R. Emerson<sup>2</sup>, and J. M. Reese<sup>3</sup>

<sup>1</sup>*Institute of Mechanics, BASci., Acad. G. Bonchev Str., Bl. 4, Sofia 1113, Bulgaria*

<sup>2</sup>*Centre for Microfluidics and Microsystems Modelling, CCLRC Daresbury Laboratory, Daresbury, Warrington WA4 4AD, UK*

<sup>3</sup>*Department of Mechanical Engineering, Strathclyde University, Glasgow G1 1XJ, UK*

**Abstract.** This paper investigates velocity inversion in rarefied cylindrical Couette flow at the two extremes of the Knudsen number regime. For low Knudsen numbers, velocity inversion is independent of the accommodation coefficient of the inner cylinder and will only occur when the accommodation coefficient of the outer cylinder lies below a critical value. It is shown that this critical value depends upon the Knudsen number and the ratio of the outer and inner cylinders. In addition, velocity inversion is also investigated in the free-molecular and near free-molecular regimes. For the specific case of specular reflection at the outer cylinder, the present study has identified two distinct categories of molecules within the flow. The first category consists of particles that collide alternately with the inner and outer cylinders whilst the second consists of particles that never collide with the inner cylinder. It is shown that recognizing these different categories of particles is the key to understanding the velocity inversion process in the near free-molecular flow regime. Finally, for large but finite Knudsen numbers, our DSMC simulations demonstrate that velocity inversion does occur provided the accommodation coefficient of the outer cylinder is sufficiently small.

**Keywords:** Velocity inversion, accommodation coefficient, cylindrical Couette flow, rotating cylinders.

**PACS:** 47.45.-n, 47.45.Gx, 47.45.Dt.

## INTRODUCTION

The phenomenon of velocity inversion in cylindrical Couette flow was first recognized by Einzel, Panzer and Liu (EPL) [1] during the development of a generalized slip-velocity boundary condition for incompressible flow over curved or rough surfaces. EPL specifically considered liquid helium and analyzed the flow using the concept of a *slip length*. In the case of a stationary outer cylinder and a rotating inner cylinder, they showed that for large values of slip length, the velocity profile becomes “inverted” with the velocity *increasing* from the rotating inner wall to the stationary outer wall. This effect was completely unexpected and contrary to the usual monotonically-decreasing velocity profile in cylindrical Couette flow.

Tibbs *et al.* [2] subsequently re-evaluated EPL’s analysis for a rarefied gas using Maxwell’s slip-velocity boundary condition and demonstrated that velocity inversion could only occur for small values of accommodation coefficient. Results from their direct simulation Monte Carlo (DSMC) method showed that the velocity profiles predicted by the slip-velocity formulation were generally in good agreement with the DSMC data. Tibbs *et al.* also demonstrated that at a Knudsen number of 0.5 and a Mach number of 0.3, density and thermal variations between the cylinders were negligible, suggesting that compressibility effects are less important for this particular problem.

The phenomenon of velocity inversion has also been investigated by Aoki *et al.* [3] using a variety of techniques including DSMC, a direct numerical solution of the Boltzmann equation using the BGK approximation, and an asymptotic analytical solution at small Knudsen numbers. Aoki *et al.*’s results reconfirmed that velocity inversion would only occur at small accommodation coefficients and showed that the presence of inversion could be related to

a *critical accommodation coefficient*. Yoshida and Aoki [4] subsequently conducted a linear stability analysis of cylindrical Couette flow without restricting the Mach number or the Knudsen number and clarified the parameter range where the flow is stable.

Yuhong *et al.* [5] have recently demonstrated that velocity inversion in the slip-flow regime is dependent only on the accommodation coefficient of the stationary *outer* cylinder. This important result allowed Yuhong *et al.* to derive simple analytical criteria to indicate whether the velocity profile behaves normally or undergoes full or partial inversion. In addition, Myong *et al.* [6] investigated low Knudsen number cylindrical Couette flow using the Langmuir adsorption model for gas-surface molecular interactions. Using a similar analysis to that proposed by Yuhong *et al.* [5], they derived the limiting condition for the critical accommodation coefficient. In the present paper, we reassess the critical value of the accommodation coefficient in the slip-flow regime and also investigate the velocity inversion problem in the near free-molecular regime.

## CYLINDRICAL COUETTE FLOW AT LOW KNUDSEN NUMBERS

We consider low speed incompressible flow between two concentric rotating cylinders. The inner and outer cylinders have radii,  $R_1$  and  $R_2$ , and rotate at constant angular velocities,  $\omega_1$  and  $\omega_2$ , respectively. For low Knudsen number flow, it can be shown that the velocity profile between the cylinders can be written as

$$u_0(r) = ar + \frac{b}{r}, \quad (1)$$

where

$$a = \frac{A\omega_1 - B\omega_2}{(A - B)} \quad \text{and} \quad b = \frac{\omega_1 - \omega_2}{(B - A)}. \quad (2)$$

Using Maxwell's slip-velocity boundary condition, the parameters,  $A$  and  $B$ , can be derived as

$$A = \frac{1}{R_2^2} \left( 1 - \frac{(2 - \sigma_2) 2\lambda}{\sigma_2 R_2} \right) \quad \text{and} \quad B = \frac{1}{R_1^2} \left( 1 + \frac{(2 - \sigma_1) 2\lambda}{\sigma_1 R_1} \right), \quad (3)$$

where  $\sigma_1$  and  $\sigma_2$  are the tangential momentum accommodation coefficients of the inner and outer cylinders, and  $\lambda$  is the mean free path defined as  $\lambda = (\mu / p)(\pi RT / 2)^{1/2}$ .

In the present study, we restrict our attention to a rotating inner cylinder and a stationary outer cylinder, since this is the case associated with velocity inversion. For convenience, the velocity profile in Eq. (1) can be non-dimensionalized with respect to the circumferential velocity of the rotating inner cylinder, giving

$$\hat{u}_0 = \frac{u_0}{\omega_1 R_1} = \frac{A}{(A - B)} \frac{r}{R_1} + \frac{1}{(B - A) R_1 r} = \frac{1}{(A - B) R_1} \left( Ar - \frac{1}{r} \right). \quad (4)$$

As shown by Yuhong *et al.* [5], the critical accommodation coefficient of the outer cylinder can be written as

$$\sigma_{2c} = 2 \left( 1 + \frac{R_2}{\lambda} \right)^{-1}. \quad (5)$$

When the accommodation coefficient of the outer cylinder is less than this critical value, the velocity profile will either be partially or fully inverted.

Defining the Knudsen number in terms of the annular clearance between the cylinders, i.e.  $Kn = \lambda / (R_2 - R_1)$  and defining the aspect ratio of the cylinders,  $\chi = R_2 / R_1$ , allows the critical accommodation coefficient for the onset of inversion to be written as a function of  $Kn$  and  $\chi$ :

$$\sigma_{2c} = 2 \left( 1 + \frac{R_2}{\lambda} \right)^{-1} = 2 \left( 1 + \frac{\chi}{(\chi - 1)Kn} \right)^{-1} = \frac{2(\chi - 1)Kn}{(\chi - 1)Kn + \chi}. \quad (6)$$

An alternative formulation for the critical accommodation coefficient was proposed by Aoki *et al.* [3]. Using a linearized BGK model they found that for small  $Kn$ , the critical value of the accommodation coefficient can be expressed as

$$\sigma_{2c} = \frac{\pi}{2} \left( \frac{R_1}{R_2} \right) \gamma_1^* Kn_{Aoki}, \quad (7)$$

where  $\gamma_1^*$  is a constant depending on the molecular model and  $Kn_{Aoki}$  is the Knudsen number defined using the radius of the inner cylinder (i.e.  $Kn_{Aoki} = \lambda / R_1$ ). Recasting Eq. (7) in terms of the Knudsen number based on the annular clearance,  $R_2 - R_1$ , leads to

$$\sigma_{2c} = \frac{\pi}{2} \gamma_1^* \frac{(\chi - 1)Kn}{\chi}. \quad (8)$$

For the hard-sphere model,  $\gamma_1^* = 1.270042$  [3].

Figure 1 compares the critical accommodation coefficient predicted by the Navier-Stokes slip-flow solution, Eq. (6), the linearized Boltzmann solution, Eq. (8), and DSMC simulations. In the present study, we have adopted the standard DSMC algorithm originally proposed by Bird [7] except for a small modification in the calculation of the maximum collision number in a cell (see Stefanov *et al.* [8]). The simulations considered a hard-sphere model for argon at STP conditions and assumed the circumferential velocity of the inner cylinder was  $V_1 = 0.3(2RT_0)^{1/2}$ . Figure 1 shows that the predicted critical values from the Navier-Stokes solution and the linearized Boltzmann solution agree with the DSMC data for  $Kn \leq 0.1$  but increasingly deviate from the DSMC data at higher Knudsen numbers. However, it is interesting to note that the linearized Boltzmann solution indicates that the critical accommodation coefficient varies linearly with Knudsen number whereas the Navier-Stokes slip-flow solution actually predicts a nonlinear variation.

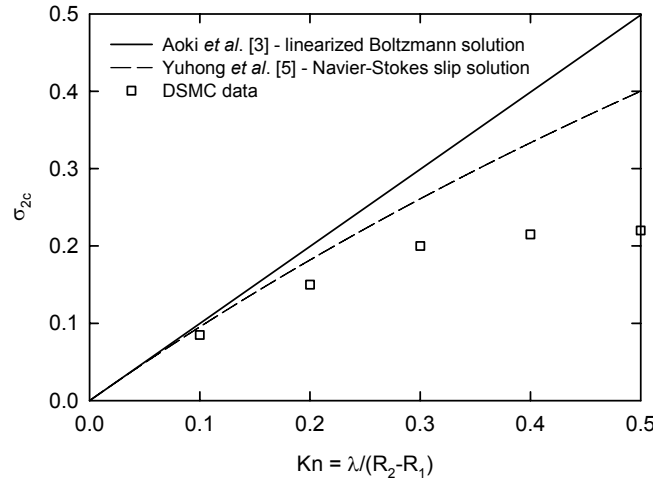


**FIGURE 1.** Comparison of the critical accommodation coefficient for the onset of velocity inversion in cylindrical Couette flow:  $\chi = R_2 / R_1 = 2$ .

## CYLINDRICAL COUETTE FLOW AT LARGE KNUDSEN NUMBERS

Aoki *et al.* [3] considered the case where the Knudsen number was infinitely large, i.e. in the free-molecular regime. They derived a solution for free-molecular flow that was valid for all accommodation coefficients with the exception of  $\sigma_2 = 0$ . In addition, Aoki *et al.* numerically investigated the flow behavior at  $Kn = 100$  to characterize the asymptotic limit of  $Kn \rightarrow \infty$ . They considered a range of accommodation coefficients, from 0.01 to 1, but only investigated cases where the inner and outer values were the same (i.e.  $\sigma = \sigma_1 = \sigma_2$ ). Under this specific condition, the free-molecular solution does not depend on the accommodation coefficient. Their numerical results were generally in good agreement with the analytical free-molecular solution. However, at low values of  $\sigma$ , there is a significant discrepancy between the numerical predictions and the analytical solution. Moreover, at  $Kn = 100$ , their results showed no evidence for an inverted velocity profile. Based upon Yuhong *et al.*'s analysis [5], it is believed that the limit  $Kn \rightarrow \infty$  needs to be reassessed for the condition  $\sigma_1 > 0$  and  $\sigma_2 \rightarrow 0$ . Under these conditions, we believe

that velocity inversion will occur for any large but finite Knudsen number provided the accommodation coefficient of the outer cylinder is sufficiently small.

### Free-Molecular Solution for $\sigma_2 = 0$

The solution in the collisionless limit ( $Kn \rightarrow \infty$ ) can be obtained by solving the Boltzmann equation with the collision integral term set to zero. In cylindrical  $(r, \theta, z)$  coordinates, the Boltzmann equation can be written in non-dimensional form [4] as follows

$$\frac{\partial \hat{f}}{\partial \hat{t}} + \zeta \cos \theta_\zeta \frac{\partial \hat{f}}{\partial \hat{r}} - \frac{\zeta \sin \theta_\zeta}{\hat{r}} \frac{\partial \hat{f}}{\partial \theta_\zeta} = 0, \quad (9)$$

where the non-dimensionalized variables are scaled by

$$\hat{t} = \frac{t}{t_0}, \quad \hat{r} = \frac{r}{L}, \quad \hat{\zeta} = \frac{\xi}{\sqrt{2RT_0}}, \quad \hat{\rho} = \frac{\rho}{\rho_0}, \quad \hat{T} = \frac{T}{T_0}. \quad (10)$$

For ease of presentation, the symbol  $\hat{\cdot}$  will be omitted from here onwards. Equation (9) has been modified by a change of variables, where  $\zeta = |\boldsymbol{\zeta}|$  and  $\theta_\zeta$  are the new variables in velocity space with  $\zeta_r = \zeta \cos \theta_\zeta$  and  $\zeta_\theta = \zeta \sin \theta_\zeta$ . The reference time is equal to  $t_0 = L(2RT_0)^{-1/2}$ . For the case of different accommodation coefficients,  $\sigma_1$  and  $\sigma_2$ , the boundary conditions on the cylinders are given by

$$f(t, R_1, \zeta, \theta_\zeta, \zeta_z) = (1 - \sigma_1)f(t, R_1, \zeta, -\theta_\zeta, \zeta_z) + \sigma_1 \frac{\rho_1}{\pi^{3/2}} \exp[-\zeta^2 + 2\zeta V_1 \sin \theta_\zeta - V_1^2 - \zeta_z^2], \quad \theta_\zeta > 0 \quad (11)$$

and

$$f(t, R_2, \zeta, \theta_\zeta, \zeta_z) = (1 - \sigma_2)f(t, R_2, \zeta, -\theta_\zeta, \zeta_z) + \sigma_2 \frac{\rho_2}{\pi^{3/2}} \exp[-\zeta^2 - \zeta_z^2], \quad \theta_\zeta < 0. \quad (12)$$

The constants,  $\rho_1$  and  $\rho_2$ , are computed from expressions for the corresponding incident number fluxes (see for example ref. [3]). In the present study, we are interested in the solution of Eq. (9) for the case of  $\sigma_2 = 0$ . To proceed, the initial state of the system is defined as follows:

$$f(0, r, \zeta, \theta_\zeta, \zeta_z) = f_0(r, \zeta, \theta_\zeta, \zeta_z). \quad (13)$$

For  $\sigma_2 = 0$  and  $t \rightarrow \infty$ , the exact solution of Eq. (9) then takes the form:

$$\left. \begin{aligned} f(r, \zeta, \theta_\zeta, \zeta_z) &= \sigma_1 \frac{\rho_1}{\pi^{3/2}} \exp[-\zeta^2 + 2\zeta r V_1 \sin \theta_\zeta - V_1^2 - \zeta_z^2], \\ &\quad (0 \leq |\theta_\zeta| \leq \varphi) \vee (\pi - \varphi \leq |\theta_\zeta| \leq \pi) \\ f(r, \zeta, \theta_\zeta, \zeta_z) &= f_0(r, \zeta, \theta_\zeta, \zeta_z), \\ &\quad (\varphi < |\theta_\zeta| < \pi - \varphi) \end{aligned} \right\} \quad (14)$$

where  $\varphi = \sin^{-1}(r/R_1)$ .

The solution consists of two non-overlapping parts with one depending on the initial state. In other words, there are two non-interacting classes of particles with distinct velocity distribution functions. The situation can be explained by considering the two different categories of particle trajectories presented in Fig. 2. The first class, depicted in Fig. 2(a), consists of particles that collide with the inner cylinder. They travel entirely in cones given by  $(0 \leq |\theta_\zeta| \leq \varphi) \vee (\pi - \varphi \leq |\theta_\zeta| \leq \pi)$ . For  $r = R_2$ , this is represented in Fig. 2(a) by a single cone. Class A has the property that each particle collides with the inner and outer cylinders alternately. In contrast, the second class of particle, illustrated in Fig. 2(b), consists of those that never collide with the inner cylinder. The main feature of class B is that the particle velocity distribution is invariant with time due to the specular reflection on the outer cylinder and is governed solely by the initial velocity distribution within the given angular interval.

It should be noted that the free-molecular solution, Eq. (14), is only valid for specular reflection at the outer cylinder (i.e.  $\sigma_2 = 0$ ). When  $\sigma_2 > 0$ , the solution previously obtained by Aoki *et al.* [3] is valid. In the next section, the free-molecular solution is used to consider the case of near free-molecular flow with  $\sigma_2 \rightarrow 0$  at large but finite Knudsen numbers.

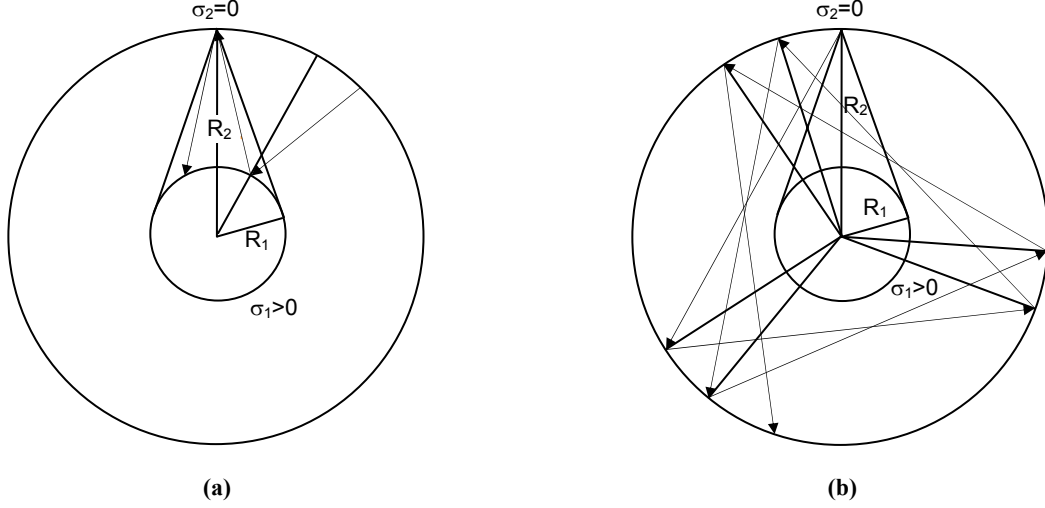


**FIGURE 2.** Schematic representation of the two types of particle motion: (a) particles in class A travel between both cylinders and always collide with the inner cylinder after being reflected from the outer cylinder; (b) particles in class B never hit the inner cylinder and are always reflected specularly from the outer cylinder.

### Near Free-Molecular Flow for $\sigma_2 \rightarrow 0$

At large but finite Knudsen numbers, the collision frequency is small but non zero. We consider the case of specular reflection on the outer cylinder ( $\sigma_2 = 0$ ) and assume  $\sigma_1 > 0$ . It is important to consider what happens to the two distinct classes of particles. During the intervals between collisions, the particle classes remain unchanged. However, after each binary collision, the interacting particles may change their class and therefore the two categories are not totally independent of each other. The intermolecular collisions give rise to friction between the classes which start transforming according to the rotation of the inner cylinder. Since there is no friction on the outer cylinder, the classes will continuously change until the friction between them disappears. In terms of the shear stress, the transformation will be complete when the shear stress is zero everywhere in the annular gap. It can be concluded that the only possible state, in this case, is a solid body rotation, leading to an inverted velocity profile. To determine the validity of this conclusion, DSMC simulations have been carried out with  $\sigma_2 = 0$  for  $Kn = 100$  and  $Kn = 1000$ . It has been found that the velocity profile is always fully inverted when  $\sigma_2 = 0$ . A series of DSMC calculations (summarized in Table 1) were performed to find the critical accommodation coefficient,  $\sigma_{2c}$ , when the velocity profile becomes partially inverted.

**TABLE 1.** Critical accommodation coefficient at large Knudsen numbers for  $\chi=2$ .

Knudsen number	Critical accommodation coefficient	Error interval
100	0.0070	$\pm 0.0005$
1000	0.00027	$\pm 0.00002$

From Table 1 it can be seen that for large Knudsen numbers, the corresponding critical accommodation coefficients are very small and decrease as  $Kn \rightarrow \infty$ . It is apparent that for an arbitrarily large but finite Knudsen number, a critical accommodation coefficient ( $\sigma_{2c} \neq 0$ ) will exist with  $\sigma_{2c} \rightarrow 0$  as  $Kn \rightarrow \infty$ . The second important finding of the DSMC study is that the time,  $t$ , required to reach a steady inverted velocity profile, after starting from a Maxwellian equilibrium velocity distribution, is very large with  $t \rightarrow \infty$  as  $Kn \rightarrow \infty$ . Figure 3 shows a typical evolution of the velocity profile against time for  $Kn = 1000$ .

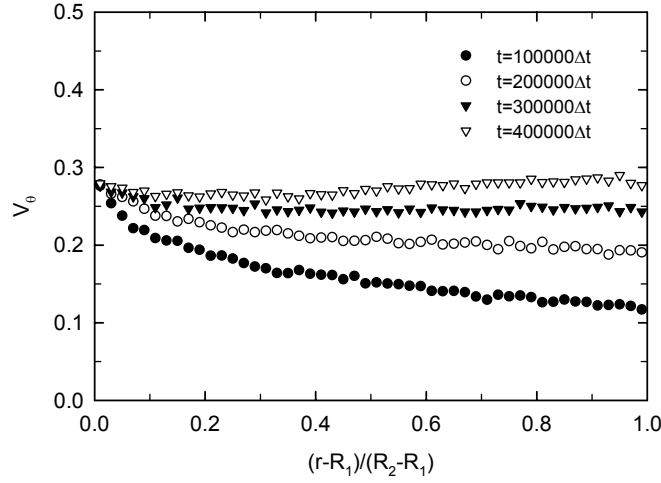


**FIGURE 3.** Evolution of the tangential velocity profile for  $Kn=1000$ . The velocity of the inner cylinder,  $V_1 = 0.3(2RT_0)^{1/2}$ ,  $\chi = 2$ ,  $\sigma_1 = 1$ ,  $\sigma_2 = 0.0001$  and the time step for the DSMC simulations is  $\Delta t = 0.5\Delta r(2RT_0)^{-1/2}$ . The cell-size is equal to  $\Delta r = (R_2 - R_1)/N_c$  where  $N_c$  is the number of cells. In this example,  $N_c = 50$ .

## CONCLUSIONS

Slip-continuum and DSMC models have been used to predict the onset of velocity inversion in rarefied cylindrical Couette flow. It has been shown that both the Navier-Stokes slip-flow solution and a linearized Boltzmann solution can accurately predict the critical accommodation coefficient for  $Kn \leq 0.1$ . Beyond the slip-flow regime, it is shown that the analytical solutions for the critical accommodation coefficient increasingly deviate from the DSMC predictions. In addition, velocity inversion is also investigated in the free-molecular and near free-molecular regimes. The DSMC simulations indicate that it is possible to obtain inverted velocity profiles at arbitrarily-large Knudsen numbers provided the accommodation coefficient of the outer cylinder is sufficiently small. The present study has also demonstrated the importance of accounting for two distinct categories of molecules within the flow. The first category consists of particles that collide alternately with the inner and outer cylinders whilst the second consists of particles that never collide with the inner cylinder. Recognizing these different particle trajectories is the key to understanding the velocity inversion process in the near free-molecular flow regime.

## ACKNOWLEDGMENTS

The authors would like to express their gratitude to the U.K. Engineering and Physical Sciences Research Council (EPSRC) for their support under grant GR/S77196/01. The first author (S. K. Stefanov) would also like to thank the Bulgarian Ministry of Education and Science for support under Grant MM1404/04. Additional support was provided by the EPSRC under the auspices of Collaborative Computational Project 12 (CCP12).

## REFERENCES

1. D. Einzel, P. Panzer, and M. Liu, *Phys. Rev. Letters* **64**, 2269-2272 (1990).
2. K. W. Tibbs, F. Baras, and A. L. Garcia, *Phys. Rev. E* **56**, 2282-2283 (1997).
3. K. Aoki, H. Yoshida, T. Nakanishi, and A. L. Garcia, *Phys. Rev. E* **68**, 016302 (2003).
4. H. Yoshida and K. Aoki, *Phys. Rev. E* **73**, 021201 (2006).
5. S. Yuhong, R. W. Barber, and D. R. Emerson, *Physics of Fluids* **17**, 047102 (2005).
6. R. S. Myong, J. M. Reese, R. W. Barber, and D. R. Emerson, *Physics of Fluids* **17**, 087105 (2005).
7. G. A. Bird, *Molecular Gas Dynamics and the Direct Simulation of Gas Flows*, Clarendon Press, Oxford (1994).
8. S. Stefanov, P. Gospodinov, and C. Cercignani, *Physics of Fluids* **10**, 289-300 (1998).